Check for updates

RESEARCH ARTICLE

The inclusion of immediate and lagged climate responses amplifies the effect of climate autocorrelation on long-term growth rate of populations

Sanne M. Evers[1,2] ⬛ | Tiffany M. Knight[1,2,3] ⬛ | Aldo Compagnoni[1,2] ⬛

[1]Department of Community Ecology, Helmholtz Centre for Environmental Research-UFZ, Halle (Saale), Germany

[2]German Centre for Integrative Biodiversity Research (iDiv) Halle-Jena-Leipzig, Leipzig, Germany

[3]Institute of Biology, Martin Luther University Halle-Wittenberg, Halle (Saale), Germany

Correspondence
Sanne M. Evers
Email: sanne.evers@idiv.de

Funding information
Alexander von Humboldt-Stiftung; Deutsche Forschungsgemeinschaft, Grant/Award Number: FZT 118; Helmholtz-Gemeinschaft

Handling Editor: Cynthia Chang

Abstract

1. Climate variability will increase with climate change, and thus it is important for population ecologists to understand its consequences for population dynamics. Four components are known to mediate the consequences of climate variability: the magnitude of climate variability, the effect size of climate on vital rates, covariance between vital rates and autocorrelation in climate. Recent studies have pointed to a potential fifth component: vital rates responding to climate in different timeframes, with some responding more immediately and some having lagged responses.

2. We use simulations to quantify how all five components modify the consequences of climatic variability on long-term population growth rates across a range of life histories defined by life expectancy and iteroparity. We use an established method to compose Matrix Population Models for 147 life histories.

3. Our simulations show that including different timeframes for vital rates responses to climate can either reduce or amplify the negative influence of climate variability on long-term population growth rates. The negative effect of different timeframes for vital rates responses on population growth is amplified when climatic autocorrelations are negative, and when species are long-lived.

4. *Synthesis.* The existing literature shows that vital rates often respond to climate in different timeframes, and that studies often ignore climate autocorrelation. Our results show that simultaneously including both of these factors can substantially increase or decrease a population's expected growth rate. Moreover, the relative magnitude of this change increases with the generation time of a life history. Our results are relevant to conservation, population forecasts and population modelling in general.

KEYWORDS
climate autocorrelation, climate drivers, degree of iteroparity, lagged climate, life expectancy, matrix population models, plant–climate interactions, stochastic population growth rate, time windows

1 | INTRODUCTION

In recent years, the threat of climate change to both plant and animal populations has become a central topic in ecology (Clark et al., 2001; Urban et al., 2016). Climate variability is projected to increase in the future (IPCC, 2014), and studies suggest that this could pose a larger threat to populations than changes in mean climate (e.g. Vasseur et al., 2014). Thus, it is important to understand how climate variability influences the vital rates (survival, reproduction, etc.) of species, their annual population growth rate (λ) and their long-term stochastic population growth rate (λs; Barraquand & Yoccoz, 2013; Lewontin & Cohen, 1969). The literature has examined four components that influence the effect of climate variation to long-term population growth: (1) the magnitude of climate variability (Boyce et al., 2006), (2) the susceptibility of vital rates to climate, in particular vital rates with high sensitivity (Morris et al., 2008), (3) the covariances among vital rates (Iles et al., 2019) and (4) the environmental autocorrelation in the climate (Fey & Wieczynski, 2017). Recent studies identified a fifth component that could affect long-term population growth: the timeframe in which vital rates respond to climate drivers (Evers et al., 2021). For example, some vital rates might respond almost immediately while others have lagged responses to climate drivers. We do not know how much temporally varied responses (TVRs; i.e. the fifth component) influence long-term population growth. It is also unclear what the relative effect and importance of the first four components are in the presence of TVRs.

Climate variability (component 1) and the susceptibility of a species' vital rates to climate (component 2) play a large role in determining the interannual variation in λ. The higher the interannual variation in λ, the lower the λs (Lewontin & Cohen, 1969; Tuljapurkar, 1990). As a result, populations for which sensitive vital rates (vital rates that strongly influence λ, Caswell, 2001) respond strongly to climate drivers are expected to change the most from increases in climate variance (e.g. Boyce et al., 2006). Covariation among vital rates (component 3) can mediate climatic effects. In particular, positive covariation increases, while negative covariation dampens, interannual variation in λ, and thus decreases and increases λs, respectively (Doak et al., 2005). In the context of climate drivers, positive covariation arises if all vital rates respond in the same direction to a certain climate driver, whereas negative covariation arises when two (or more) vital rates respond in opposite directions to the same climate driver.

The environmental autocorrelation in climate (component 4), in which the climate at each point in time is correlated to the previous environment, also influences interannual variation in λ and extinction risk. Positive environmental autocorrelation tends to increase extinction risk because populations in decline tend to stay in decline. On the other hand, negative environmental autocorrelation tends to stabilize populations, as declines are followed by increases (Heino & Sabadell, 2003; Pilowsky & Dahlgren, 2020; Schwager et al., 2006). The effect of environmental autocorrelation generally has a small effect on population growth rates when compared to the effects of other components, such as vital rate covariation (e.g. Morris et al., 2011). However, environmental autocorrelation can be important for species that recover slowly from perturbations (Tuljapurkar & Haridas, 2006), such as those with long lifespans and high reproductive output (Salguero-Gómez et al., 2016).

The fifth component, when different vital rates respond to climate drivers in different timeframes (TVRs), has been shown to occur by recent research that considers climate timeframes other than the typical first 12 months prior to vital rate responses (Evers et al., 2021; Tei et al., 2017; Tenhumberg et al., 2018). Here, we show that TVR and climate autocorrelation affect λs via their effect on vital rates covariations. For example, consider a species with two vital rates that respond positively to the same climate driver. In the absence of TVR, the correlation between the vital rates will be strongly positive. However, in the presence of TVR (e.g. survival responds to climate in the current year, and fecundity responds to climate in the previous year), the correlation between the vital rates will depend on the temporal autocorrelation of the climatic driver. Specifically, strong negative autocorrelation will produce a strong negative vital rate covariation, thus increasing λs; vice versa for a strong positive autocorrelation.

We also expect that life history of a species will influence the extent to which TVR will influence populations growth rate. Species with low life expectancies typically have low juvenile survivorship, and species with high iteroparity typically have high adult survivorship. When the means of survivorship are close to zero or to one, high coefficients of variation are not possible (Morris & Doak, 2004), and we expect the effects of TVR to diminish in magnitude. This leads us to the expectation that the relative effects of TVR will vary with life history (e.g. longevity and parity).

Here, we use simulations to investigate how the five components we described above mediate the effect of climate variation on λs. We simulate matrix population models that represent a wide range of life histories. We then run stochastic simulations in which TVR is either present or absent, while modifying the first four components (climate variability, climate effect strength, vital rate covariation and climatic environmental autocorrelation). By doing so, we elucidate how long-term viability responds to TVR across a large range of life histories.

2 | MATERIALS AND METHODS

To investigate the effect of TVR on long-term population growth rate across a broad range of life histories, we used a well-established framework to create Matrix Population Models (MPMs) representing a wide range of life histories (Neubert & Caswell, 2000). We use these MPMs to conduct stochastic simulations of their dynamics under different scenarios of environmental autocorrelation, environmental variance, strength of climatic signal, vital rate covariation and TVR (Figure 1).

2.1 | Simulating temporal sequences

We simulated variation in the vital rates of MPMs starting from normally distributed environmental sequences (V) with standard deviation σ_V. These environmental sequences reflect the response of a vital rate to both a climate driver, C, and unexplained environmental

Simulating temporal sequence

(a) Climate autocorrelation (r_K)
−0.6   0.6

Climate standard deviation (σ_V) 0.1 0.5

Population models across life histories

(b)
$$A_i = \begin{pmatrix} S_{J,i}(1-\gamma) & \varphi_i \\ S_{J,i}\gamma & S_{A,i} \end{pmatrix}$$

ID	γ	S_J	S_A	φ
60	0.5	0.5 (0.23)	0.2 (0.35)	2.4 (1.43)

+ Random noise (ε)

Environmental sensitive Matrix Population Models

(c)
For timestep (i) = 10

$v_{recent,10} = -0.55$
Prob = 0.138

$v_{lagged,10} = 1.09$
Prob = 0.985

Variance transfer Quantile calculations

$S_{J,10} = 0.72$

$S_{A,10} = 0.62$

$\varphi_{10} = 1.32$

(d) Repeat for $i = 1{:}10{,}000$

$$A_{10} = \begin{pmatrix} 0.72(1-0.5) & 1.32 \\ 0.72 * 0.5 & 0.62 \end{pmatrix}$$

(e) Calculate stochastic log lambda (λ_s) from A-sequence

(f)

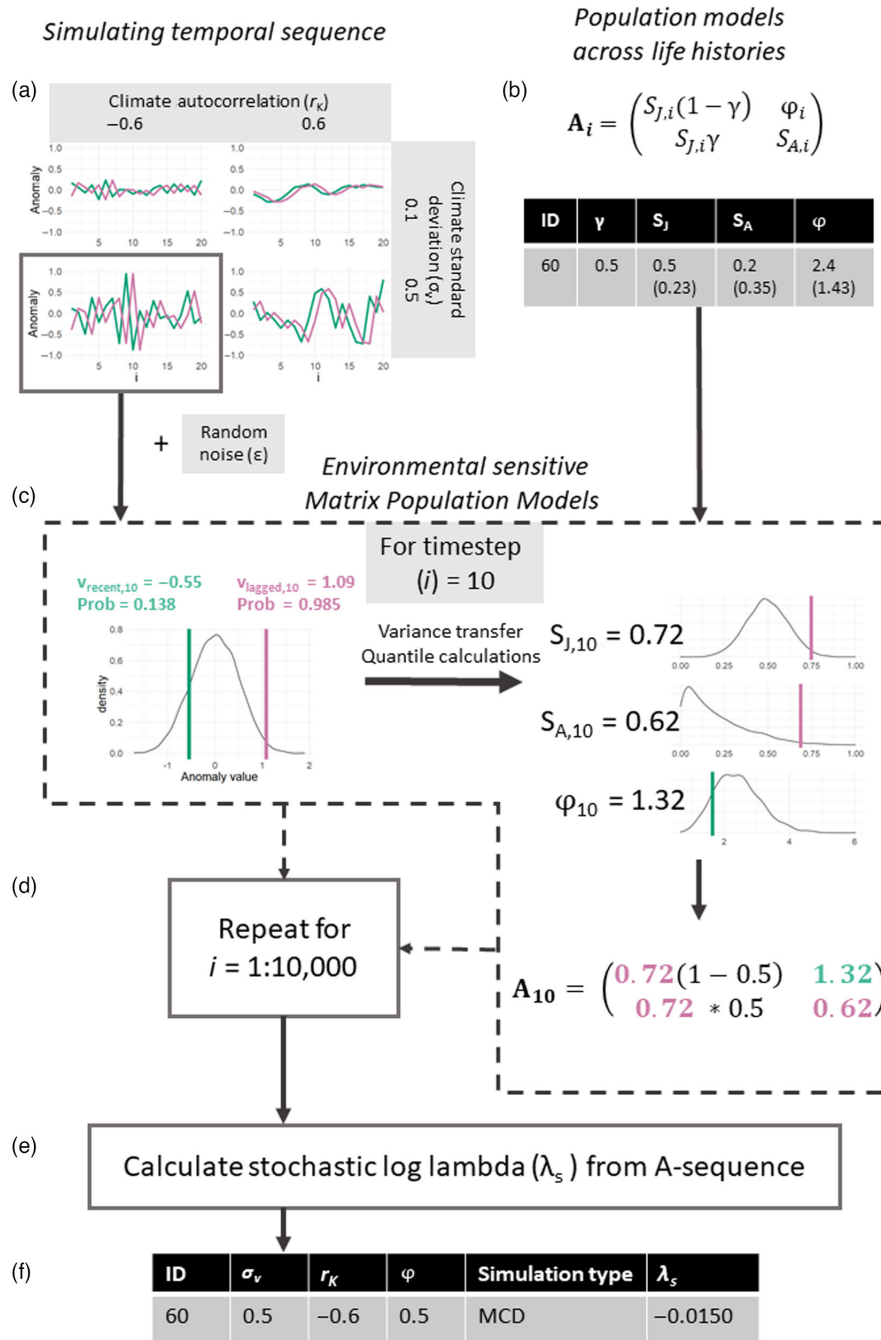| ID	σ_v	r_K	φ	Simulation type	λ_s
60	0.5	−0.6	0.5	MCD	−0.0150

FIGURE 1 Workflow to simulate the effect of climate autocorrelation (r_K), climate variability (standard deviation of its distribution, σ_C), signal strength (p) and temporally variable response (TVR), on the stochastic natural logarithm of population growth rate (λ_s). (a) Create climate sequences of 10,000 steps, with different levels of autocorrelation and σ_c, and combine them with random noise into an environmental sequence (in this example, 50% climate signal, 50% noise, signal strength=0.5). (b) Using a 2×2 MPM, create 147 different life histories, with different values for transition probability from juvenile to adult (γ), juvenile and adult survival (S_J and S_A), and with fecundity (φ) set so that matrix A produces a stable population (population growth rate=1). As an example, one life history (ID) can be seen in the table, with vital rate means and standard deviations (in parentheses, for the three fluctuating vital rates). (c) For each time step, here as example $i=10$, calculate the quantile probability of the recent and one-step lagged value from the normally distributed temporal sequence from (a), given a mean of 0 and standard deviation of σ_c. Using this quantile probability, calculate the corresponding quantiles on the beta (for vital rates S_J and S_A) and gamma (for vital rate φ) distributions given the vital rates' respective mean and standard deviation defined in (b) to populate the A_i matrix. (d) Repeat these calculations for all steps in the sequence. (e) Calculate the λ_s using the sequence of A matrices. (f) Create the result table with λ_s for each of the different life histories, autocorrelation, climate variability, signal strengths and simulation type (TVR) as shown here, or control where φ also responds to recent climate (in green).

variation represented as random noise, ε (Figure 1a). We control the environmental variance (V) explained by climate (C) using signal strength (p). Signal strength varies between 0 and 1, where, for example, 0.5 and 1 imply that climate explains, respectively, 50% and 100% of the environmental variance σ_V^2. We then converted these normally distributed sequences to the beta and gamma distributions that characterize the survival and fecundity rates, respectively (see Section 2.3 below, Figure 1c).

We simulated the environmental sequences (V) by adding two separate random processes: the climate sequence (C) and the unexplained variation (ε). We first simulated climate sequences, C, using 35 combinations of standard deviation and autocorrelation (see S1.1 for detailed methods). We included five levels of the environmental standard deviation, σ_V (0.01, 0.258, 0.505, 0.753 and 1). We chose these values to scale standard deviation of vital rates (see 'Population Models across life histories') from 1 to 100% (component 1). We incorporated seven levels of autocorrelation in the climate sequences (component 4): −0.6, −0.3, −0.1, 0, 0.1, 0.3 and 0.6. For each combination of σ_V and autocorrelation ($N = 35$ combinations), we simulated 30 different sequences, resulting in 1050 climate sequences.

The final step to produce the environmental sequence, V, was to simulate random noise (ε), partition the variance of C and ε, and add them together. We included random noise in the temporal sequences to represent other factors that influence population dynamics in the real world, such as anthropogenic disturbances, biotic interactions or other unknown climate drivers. We computed each individual value, i, of this temporal sequence, V, as

$$V_i = C_i * \theta_p + \varepsilon_i * \theta_{1-p}, \tag{1}$$

where ε_i is the ith individual random deviate from a normal distribution with mean 0 and standard deviation σ_V, C_i is the ith random deviate from climate sequence described above with mean 0, standard deviation σ_C, and an autocorrelation level. We multiply each random deviate C and ε_i by parameters θ_p and θ_{1-p} to control the proportion (p) of variance in V that is explained by the climate driver C; p can also be seen as the signal strength of C, or the susceptibility of the vital rates to the climate driver C. Because our objective is to produce an environmental sequence V with standard deviation σ_V, summing up C and ε with untransformed variance σ_V^2 would produce a V with standard deviation $\sqrt{2\sigma_V^2}$. Multiplying each C_i and ε_i random deviate by θ_p and θ_{1-p}, respectively, shrinks their standard deviation to produce a V variable with the desired σ_V. For example, if the signal strength (p) is 0.5 and we aim to produce a random variable V with a standard deviation (σ_V) of 1, θ_p and θ_{1-p} are equal to approximately 0.7071. These values make intuitive sense on the variance scale: they produce two random variables C and E with standard deviation 0.7071 (and therefore variance 0.5), which sum to produce a variable V with standard deviation 1 (and therefore variance 1). We implemented four different p values (0.05, 0.25, 0.5 and 1). As such, we have temporal sequences where hardly any variance is explained by the climate driver, to sequences where the temporal sequence is fully driven by the climate driver. Our sequences thus encompass a range of temporal variance, autocorrelation and of variance explained by the climate driver.

2.2 | Population models for a range of life histories

To address how TVR (component 5) affects population demography, we used the Matrix Population Model (MPM) parameterization suggested by Neubert and Caswell (2000; Figure 1b). This MPM has two stages, juvenile and adult, and yearly transitions are described by the following equations:

$$n_{t+1} = n_t * A_t, \tag{2}$$

$$A_t = \begin{pmatrix} S_{J,t}(1-\gamma) & \varphi_t \\ S_{J,t}\gamma & S_{A,t} \end{pmatrix}, \tag{3}$$

where n_t and n_{t+1} are population size vectors at time t and $t+1$, respectively, A_t is the transition matrix, γ is the probability of transitioning from juvenile to the adult stage if the individual survives to from t to $t+1$, $S_{J,t}$ and $S_{A,t}$ represent the survival probability of juveniles and adults, respectively. Finally, φ_t is the number of offspring produced per surviving adult. This MPM can model a large range of life histories depending on the vital rate (γ, S_J, S_A and ρ) values (Neubert & Caswell, 2000). For example, changing adult survival so that it approaches 0 ($S_A \rightarrow 0$) changes the model species from iteroparous to semelparous (Neubert & Caswell, 2000). We recognize that to model the full range of life histories observed worldwide, we would need more realistic and complex MPMs. However, this simple life cycle can still span a wide range of life histories, and is sufficient to explore the relative effect of responding to different time windows on population dynamics across life histories.

To create MPMs that span a wide range of life histories, we followed Koons et al.'s (2016) method (Figure 1b). We set γ to either 0.2, 0.5 or 0.8 and set S_J and S_A from 0.05 to 0.95, in steps of 0.15. Then for every possible combination of γ, S_J and S_A, we calculated a value of φ such that Equations 2 and 3 would result in a population growth rate (λ) of 1 (which equals a stable population). This resulted in 147 different life histories. Next, we calculated the standard deviation of S_J, S_A and φ to run stochastic simulations. Most of the existing literature assumes that in real-world populations, these standard deviations evolve to inversely correlate to the elasticity of vital rates, a pattern known as 'demographic buffering' (reviewed in Hilde et al., 2020). While evidence contrary to demographic buffering exists (e.g. Jäkäläniemi et al., 2013; McDonald et al., 2017), we decided to follow Koons et al.'s (2016) method in this as well, as it reflects the more common evidence on demographic buffering. To simulate these standard deviations, we used the elasticities (e) of S_J, S_A and φ to calculate a proportional measure of buffering: $\tau_i = (1 - e_i) / \max(e_{S_J}, e_{S_A}, e_\varphi)$ where i is S_J, S_A or φ. We calculated the standard deviation of survival rate, VR, as $\sigma_{VR} = \tau_i * 0.5 * CV_{\max} * \overline{VR}$, where $CV_{\max}$ is the maximum coefficient of variation of a probability (Morris & Doak, 2004). Following Koons et al. (2016), we set $CV_{\max}$ to 1 for φ.

Finally, we calculated two life-history traits (life expectancy and degree of iteroparity, Demetrius entropy) for our 147 life histories using the POPBIO (Stubben & Milligan, 2007) and RAGE (Jones et al., 2022) R packages. To improve model fit, and facilitate

comparisons of effect sizes, we transformed ln(life expectancy) and iteroparity into *z*-scores.

2.3 | Environmental sensitive matrix population models

We then created an environmentally sensitive MPM to include the climate effect size (component 2) in our projections (Figure 1c). We kept γ fixed, but simulated variation in the other vital rates (S_J, S_A and φ) by mapping the normally distributed temporal sequence v (Equation 1) in beta-distributed (for S_t) and gamma-distributed (for φ_t) values. To do so, we calculated the quantile of each V_i value given the distribution of V, and computed the value of that quantile for the beta and gamma distributions (Figure 1c). For example, if a value of V_i was the 98th percentile of its normal distribution, we drew the 98th percentile from the beta distribution for $S_{J,t}$ and $S_{A,t}$ (see S1.2). Note that while the means of these vital rates always remained the same, we scaled standard deviations by a factor σ_V (which ranged from 0.01 to 1).

2.4 | Population projections

Using the MPMs and the environmental time series, V, we investigated the effect on populations when some of their vital rates respond to a recent climate driver, and others respond to lagged climate. Using these TVRs to climate drivers, we projected the population dynamics over 10,000 time steps (Equation 2 and 3, Figure 1d) and calculated λs using the POPBIO package (Stubben et al., 2016) in R (R Core Team, 2021). We obtained a temporal sequence from Equation 1 (hereafter, V_{recent}) and created the corresponding lagged temporal sequence by offsetting the C sequence of V_{recent} by one step, and a new ε sequence to create V_{lagged} (Figure 1a). In the 'control' simulations, S_J, S_A and φ responded to the same C sequences, but different ε sequences. In the 'TVR' simulations, the fecundity vital rate (φ) responded to V_{recent}, but the survival vital rates (S_J and S_A) responded to V_{lagged}. In these simulations, all vital rates respond in the same (positive) trend to the V sequences, thus creating positive covariance between the vital rates (component 3). Initial analysis showed that there was no difference in λs when fecundity instead of the survival responds to V_{lagged}; therefore, we only show the first.

Next, we repeated the simulations described above, but with the assumption of negative covariance (component 3) between the survival and fecundity vital rates in their response to C. Using similar calculations as described in the previous paragraph, we investigated the effect that responding to TVR could have, if the responses of the different vital rates to climate were negatively correlated. For this, we re-ran the simulations in the previous paragraph, but multiplied C_i in Equation 1 by −1 for the fecundity vital rate (φ).

In both simulations mentioned above, vital rates all respond equally strongly (p) to the climate driver. However, it is possible that stages respond with different intensity to a climate driver (e.g. Tredennick et al., 2018). Therefore, as an additional analysis, we also picked one

life history, and repeated the simulations with positive covariance. For each of the simulations, we modified the response of S_J, S_A or φ to the climate driver to be only half that of the other two vital rates. For example, in one simulation, S_J and S_A would have a $p=0.5$, and φ would have a $p=0.25$. More details on the simulations are shown in S3.

Finally, to summarize the effect sizes of the different components (climate variance, signal strength, vital rate covariance, climate autocorrelation and TVR) on λs we used linear mixed effect models for both the positive and negative vital rate covariance simulations. In these models, λs was the response variable, and the fixed effects were climate variance (σ_c; linear and quadratic), climate autocorrelation (r_K), signal strength (p), simulation type (TVR versus control) and the interaction of simulation type with σ_c, autocorrelation and signal strength (p). For the random slope, we used the effect of climate variance for each life history.

We first examine the outcome of simulations focusing on a single representative life history, and then use the linear mixed effect model to quantify the effects of fixed effects across our life histories. As our representative life history, we choose a matrix model with $S_J=0.5$, $S_A=0.2$, $\gamma=0.5$, and $\varphi=2.4$, because this life history is relatively central in both longevity and iteroparity, and because it visually clearly shows the trends found across all life histories.

2.5 | Correlation with life-history traits

We investigated how mean ln(life expectancy) and degree of iteroparity correlated with our simulation results. We first calculated the log relative decrease in λ_s from $\sigma_c=0.01$ to 1 for both the TVR and control simulations across the σ_c values. Specifically, we calculated relative decrease as

$$\text{relative decrease} = \ln\left(\frac{\lambda_{s,control,\sigma_c=1} - \lambda_{s,control,\sigma_c=0.1}}{\lambda_{s,TVR,\sigma_c=1} - \lambda_{s,TVR,\sigma_c=0.1}}\right). \quad (4)$$

Using this measure, values above zero meant that the TVR simulations had relatively lower decrease, and thus higher λ_s than control simulations. We then fit a linear mixed effect model, with the relative decrease as the response variable. The fixed effects were life expectancy, iteroparity, climate autocorrelation and signal strength, as well as the interaction between life expectancy and iteroparity with climate autocorrelation. The random effect was an intercept for each of our 147 different life histories.

3 | RESULTS

3.1 | Simulations across life histories

The results for our representative life history ($S_J=0.5$, $S_A=0.2$, $\gamma=0.5$, and $\varphi=2.4$) show three main patterns in which TVR change λ_s. First, when vital rates respond in the same direction to climate, interannual variance in λ is lower (Figure 2), resulting in higher λ_s
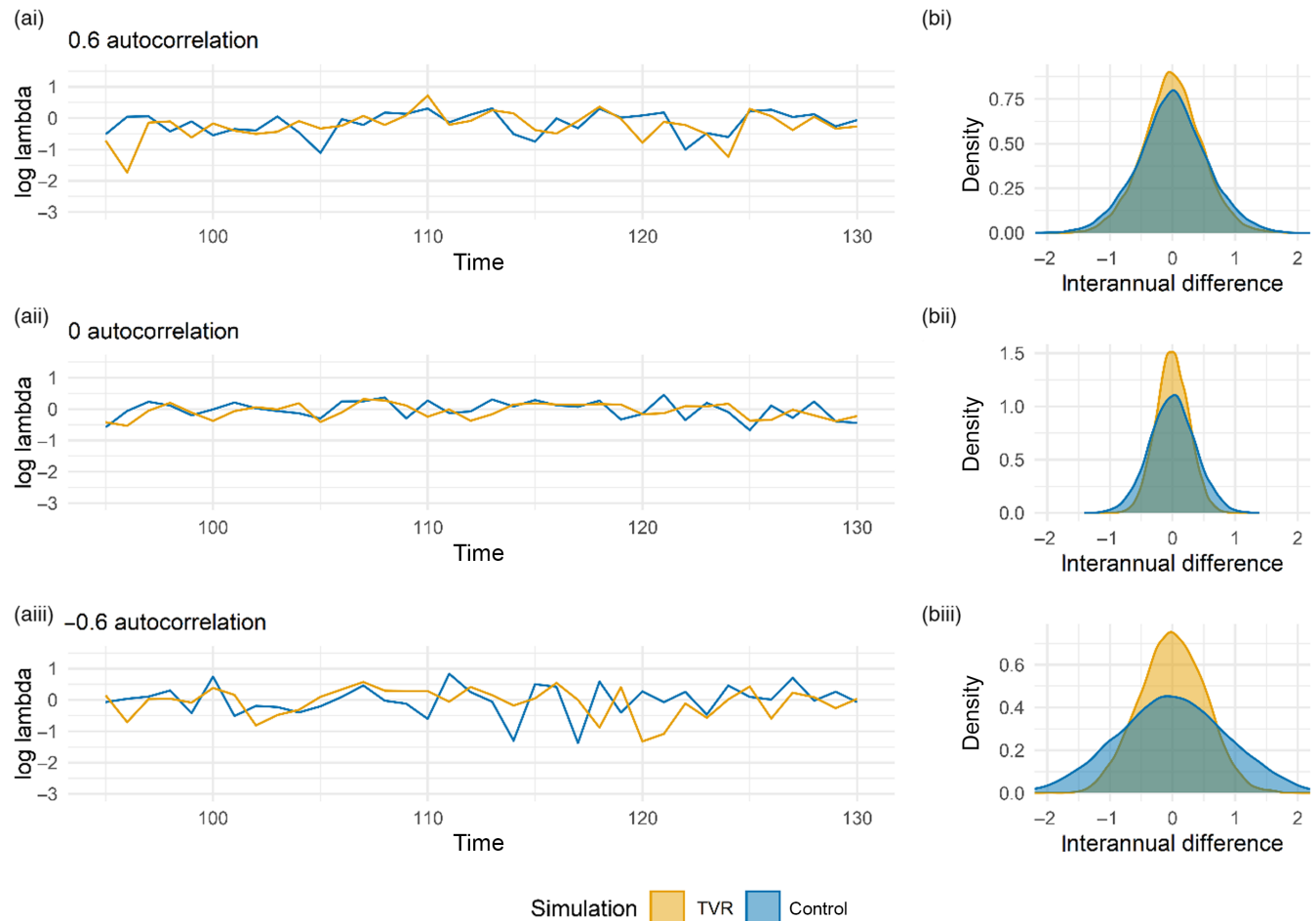
FIGURE 2 Under positive vital rate correlation, temporally varied response (TVR) simulations result in lower interannual variance in the natural logarithm of the population growth rate (log lambda) compared to the control simulation. (a) Log annual population growth rate (λ) across a 35-year time series (years 95–130 of 10,000 years) of stochastic matrix population model (MPM) projections where the MPMs vary according to a climate driver, and random noise. In this simulation, 50% of the variance was explained by a climate driver and 50% of the variance was random. In the 'control' simulation, all vital rate models respond to recent climate and in the TVR simulation, the survival vital rates (juvenile and adult survival) respond to 1-year lagged climate, whereas the fecundity vital rate responds to recent climate. Simulations were done under (i) 0.6, (ii) 0 and (iii) −0.6 environmental autocorrelation in the climate driver. (b) The density distribution of the interannual difference in λ for the whole 10,000-year sequence under (i) 0.6, (ii) 0 and (iii) −0.6 environmental autocorrelation in the climate driver.

(Figure 3a). Second, these effects of TVR are amplified for larger values of σ_c and autocorrelation (Figure 3a). Regarding autocorrelation, its direct effect is minuscule when compared to its interaction with TVR (Figure 3a,b). Third, and importantly, in the case vital rates respond in opposite direction to climate, these two effects of TVR are reversed in sign, resulting in lower λ_s values (Figure 3b).

The linear mixed effect model shows that the above patterns hold across all life histories (see S2.4 for plots on the results for every life history), and it indicates two additional patterns. First, that signal strength (p) also amplifies the effects of TVR (Figure 4) with a magnitude similar to autocorrelation and σ_c. Second, it emphasizes that environmental variance σ_c remains the predominant force controlling λ_s (Figure S2.3).

Finally, we used the same life history as in Figure 3 (S_J=0.5, S_A=0.2, γ=0.5 and φ=2.4), to investigate the effect of different climate signal strengths across vital rates. When one vital rate experiences a climate signal (p) that is only half of the climate signal experienced by the other vital rates, the trends and relationships found in the main analysis remain (see S2.2).

3.2 | Correlation with life-history traits

The largest effects of TVR simulations on stochastic population growth rate (λ_s) occur for species with high life expectancy and, to a much lesser degree, species with low degree of iteroparity (Figure 5 and S2.4). Model estimates show that these effects of life history are amplified under negative autocorrelation (r_k) (Figure 6). As seen previously, the models confirm that the sign of vital rate correlation switches the effect of TVR on λ_s from beneficial (positive correlations)
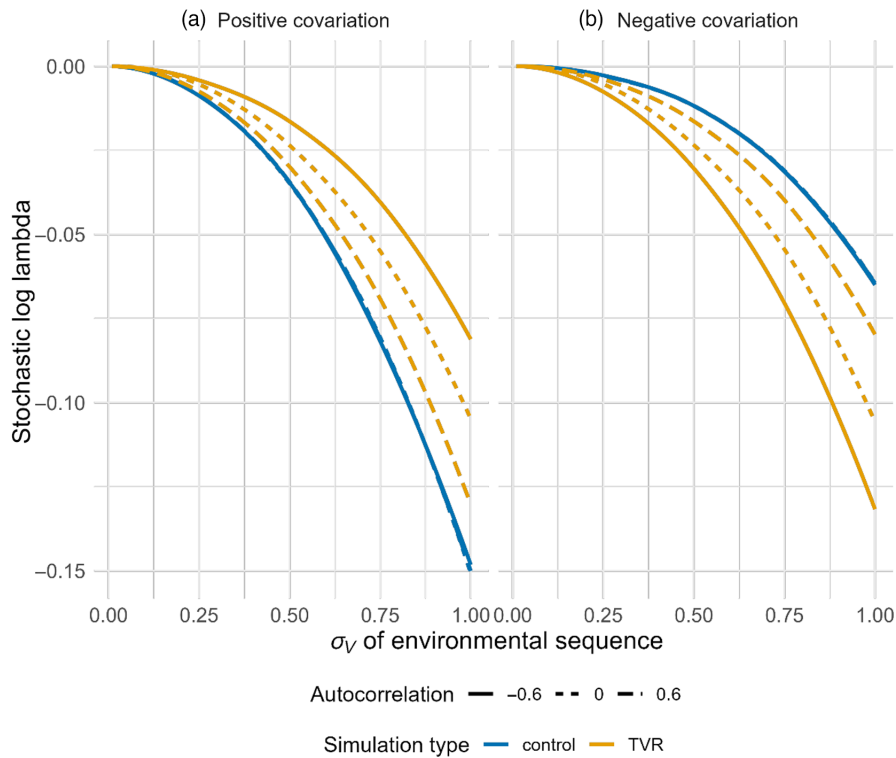
FIGURE 3 Responding to both lagged and recent climate (i.e. temporally varied responses—TVRs) can either buffer or amplify the negative effect of increasing environmental standard deviation (σ_V). Projected stochastic population growth rates of a life history over a range of environmental variation and climate autocorrelations, using a 2-by-2 matrix population model. In this simulation, 50% of the variance was explained by a climate driver and 50% of the variance was random. We included two types of simulations, the control where all vital rates respond to the same (recent) climate, and the TVR simulations, where the vital rates in the somatic submatrix (survival) respond to climate that is 1 year lagged from that of the reproductive submatrix (fecundity). In (a), all vital rates respond in a positive direction to the climate driver. In (b), the reproductive submatrix responds to the climate driver in the opposite direction of the survival submatrix.
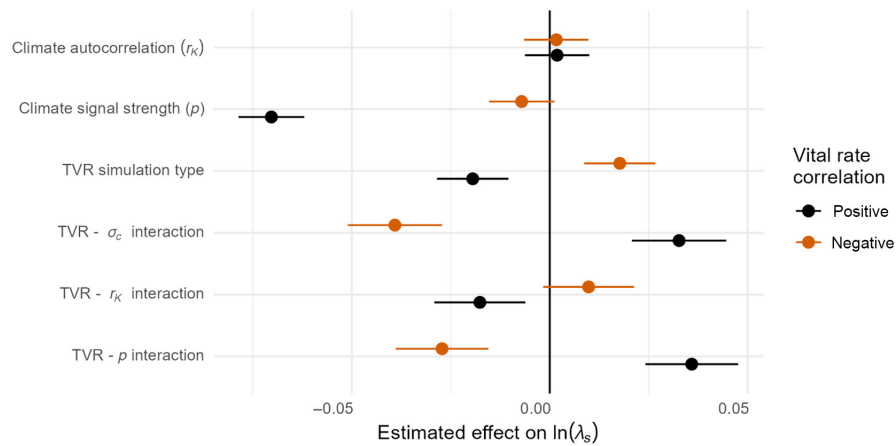
FIGURE 4 Selected coefficient estimates and 95% confidence interval of the two linear mixed effect models, relating the stochastic log lambda of population dynamic simulations to climate variables under either positive (in black) or negative (in red) correlation between the survival and fecundity vital rates. Climate autocorrelation (r_K) is the autocorrelation in the climate sequence used in the simulations, ranging from −0.6 to 0.6. Climate signal strength (p) is the relative importance of the climate sequence compared to random noise, ranging from 0.01 to 1. Temporally varied response (TVR) simulation type is the difference between the control and TVR simulations. Finally, the figure shows the estimates for the interaction effect of TVR with the climate standard deviation (σ_c), autocorrelation and signal strength, respectively. The coefficients of the linear mixed effect model not included in this graph are the intercept (positive; −0.045, −0.052:−0.038 CI; negative; −0.078, −0.085:−0.071 CI), and the linear (positive; 1.217, 1.195:1.239 CI, negative; 1.256, 1.233:1.278 CI) and quadratic (positive; −2.110, −2.664:−1.555 CI, negative; −2.077, −2.629:−1.524 CI) effects of σ_c.
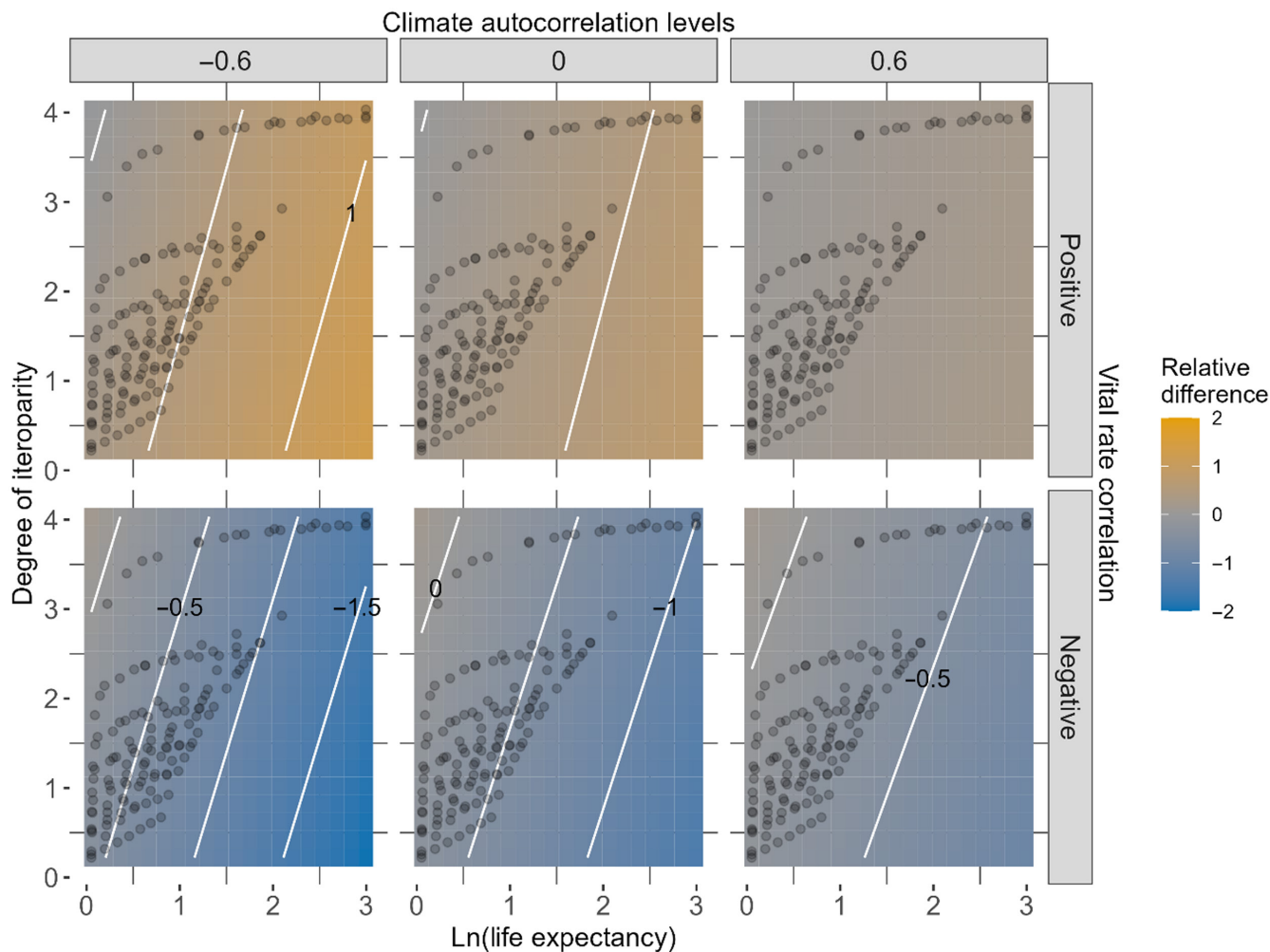
FIGURE 5 Slow life histories see the largest change in stochastic population growth rate (λ_s) in the presence of temporally varied responses (TVR). Relative difference in the decrease in stochastic population growth rate (λ_s) between simulations with TVR and control simulations, across a range of iteroparity and life expectancy. Colours show the predicted values of linear mixed effect models relating TVR to stochastic population growth rate (λ_s). Difference in λ_s was defined as the change in stochastic population growth rate from climate standard deviation of 0.1 to 1. The relative difference in λ_s was calculated by dividing the difference of the control simulations by the TVR simulations. Positive values indicate that TVR is beneficial for the population growth rate (i.e. has a lower decrease in λ_s compared to the control simulations), whereas negative values indicate that the responding with all vital rates to the same time window (control) is beneficial for the population growth rate. Each circle represents one of the 147 simulated life histories. In the TVR simulations, survival responds to climate that is 1 year lagged from that of fecundity; in the control simulations, all vital rates respond to the same (recent) climate. The results in the graphs refer to a climate signal strength of 0.5 (i.e. 50% of the vital rate's variance is driven by climate). Columns refer to three levels of autocorrelation (−0.6, 0 and 0.6). Rows refer to positive vital rate correlation (where all vital rates respond positively to the climate driver), or negative vital rate correlation (where the survival and fecundity vital rates respond in different directions to the climate driver).

to detrimental (negative correlations, Figure 6). Figure S2.2 shows a graphical comparison of different life histories on the extremes of life expectancy and degree of iteroparity.

4 | DISCUSSION

There is concern that increased climate variance poses a threat to populations, which has motivated considerable interest in understanding this topic (e.g. Boyce et al., 2006; Vázquez et al., 2017). Here, we found that when vital rates of populations respond to climate with a mix of more recent and lagged climate driver timing

(TVR), this response buffers the populations from the effects of environmental variance on population growth. In particular, this buffering effect always occurs when the vital rates of a species respond to a climatic driver in the same direction (positive covariance). The magnitude of this buffering increases in inverse proportion to the temporal autocorrelation of climatic drivers. On the other hand, in the case of opposing responses of vital rates to the climate driver, TVR could actually exacerbate the effect of increasing climate variability. These results are relevant to population and conservation ecologists for two reasons. First, our results show that the direct effects of environmental autocorrelation on population dynamics are small with respect to their potential indirect effects mediated by
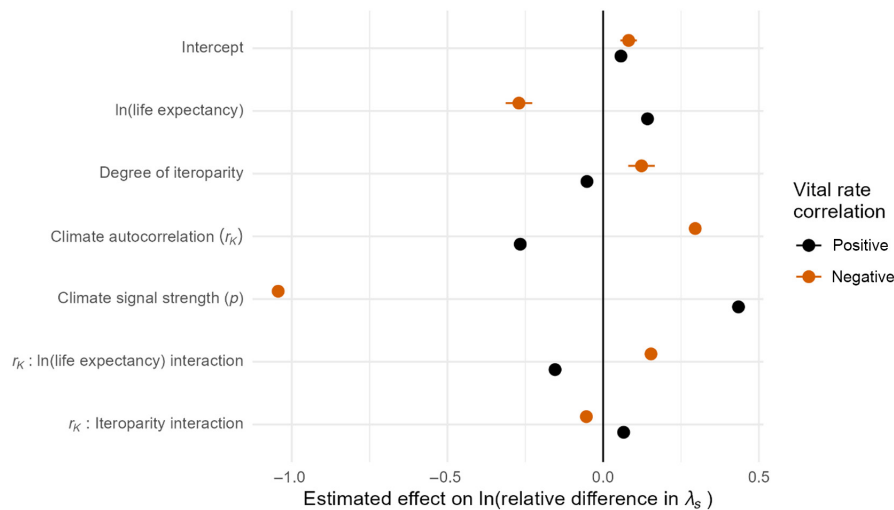
FIGURE 6 Coefficient estimates and 95% confidence interval of the two linear mixed effect models, relating the relative decrease in stochastic population growth rate to different life history and climate variables, and their interactions, under either positive (in black) or negative (in red) correlation between the survival and fecundity vital rates. ln(life expectancy) and degree of iteroparity are scaled variables for comparison. Climate autocorrelation (r_K) is the autocorrelation in the climate sequence used in the simulations, ranging from −0.6 to 0.6. Climate signal strength (p) is the relative importance of the climate sequence compared to random noise, ranging from 0.01 to 1.

TVR. Second, the conditions that lead to TVR buffering the effects of environmental variance are likely common in nature. Thus, our results encourage empirical studies to identify TVR, and to include them in population projection models.

Our results are perhaps the first to suggest that environmental autocorrelation might affect λs indirectly, by affecting vital rates covariation via TVRs. Previous studies found that environmental autocorrelation has relatively small direct effects on population growth rates (Eckhart et al., 2011; Paniw et al., 2018). As a result, many researchers currently investigate stochastic population dynamics under the assumption that no autocorrelation is present (e.g. Compagnoni et al., 2016; McDonald et al., 2017). Our simulations show that environmental autocorrelation can have up to 10 times larger an effect on λ_s through interaction with TVR, compared to its direct effect. Temporal autocorrelation is expected to increase under climate change (Di Cecco & Gouhier, 2018), which would decrease the indirect buffering effect of TVR. However, significant regional variation in trends are also expected (Di Cecco & Gouhier, 2018), including regional decreases in autocorrelation, which would actually decrease their extinction risk.

We show that the presence of TVR reduces the annual variation in lambda and thus relatively increases λs under a wide range of scenarios that are likely to occur in nature. TVR increases λs when vital rates respond in the same direction to climate drivers. Climate drivers are usually thought to cause responses in vital rates that are similar in direction (e.g. Compagnoni et al., 2021; Hindle et al., 2019). For example, drought typically harms multiple vital rates rather than harm some and benefit others. Examples of opposing trends in vital rate responses do exist (e.g. Dahlgren et al., 2016; Noël et al., 2010); however, this opposing responses do not necessarily reflect direct responses to climate, but rather physiological trade-offs that end up resulting in correlations of

opposing sign (e.g. trade-offs in vital rates in response to limited resource availability rather than a direct response to the climate driver; Crone et al., 2009; Tenhumberg et al., 2018). This benefit of TVR is highest in the presence of large, negative environmental autocorrelation. On the other hand, the benefit of TVR mostly disappears only in the presence of large, positive autocorrelation, or when the climate has a very weak effect on the temporal variance of vital rates. These conditions should also be uncommon in nature, as autocorrelations are not known to be so extreme as those considered in our simulations.

We find consistent results across life histories in the direction of the TVR effect on λs, suggesting that the effects of TVR on populations can likely be generalized to a variety of life histories. As expected, we find that the relative effects of TVR tend to be stronger in populations with high life expectancy and/or with low iteroparity. This is likely because high coefficients of variation are not possible for populations with low life expectancy (where juvenile survivorship is close to 0) or with high iteroparity (where adult survivorship is close to 1; Morris & Doak, 2004). However, the relative decrease in λs under TVR was much more severe with changing life expectancy than with changing iteroparity. This could be because TVR effects on populations with different life expectancies act primarily through effects on juvenile survivorship, and effects on this young stage class can have a cascading effect on the entire life cycle.

Based on physiological principles, we expect that many natural populations have TVR. For example, many plant species are known to have preformation of leaves and/or inflorescences more than 12 months before emergence (e.g. Diggle, 1997; Inouye, 1986). Thus, the vital rates associated with growth and/or fecundity will respond to climate drivers in this same timeframe as the preformation (e.g. Evers et al., 2021). In combination with

possible frost damage that has rapid demographic consequences (e.g. Iler et al., 2019), alpine species could be a prime example of species with TVR. The presence of below-ground rhizomes is another physiological characteristic that has been linked to lagged climate drivers in *Heliconia acuminata* (Scott et al., 2021). For this species, more immediate climate responses have been observed as well (Westerband & Horvitz, 2017). Even if species only exhibit immediate physiological responses to climate drivers, indirect climate effects can still lead to TVR. For example, the presence of nurse plants positively influenced seedling recruitment (e.g. Flores-Torres & Montaña, 2012), and any delayed effect of climate on the nurse plant would thus translate to the seedling as well.

Studies have shown that vital rates (growth, survival and reproduction) correlate with climate drivers in unique ways that reflect different biological mechanisms (Bogdziewicz et al., 2020; Fritts, 2012; Trugman et al., 2021). Therefore, it is plausible that the link between vital rates and climatic drivers is complex in nature. Currently, few empirical studies have tested for the presence of TVR. However, previous studies searching for TVR have found evidence for them (Evers et al., 2021; Scott et al., 2021; Tenhumberg et al., 2018), suggesting that TVR might be common. Our recent study (Evers et al., 2021) conducted a review of literature published between 1997 and 2017 and found that most demographic studies consider only a single climate timeframe: typically, the first 12 months prior to vital rate responses. However, among the eight studies that tested for the presence of lagged effects in multiple vital rates, seven found evidence of TVR (Evers et al., 2021).

Our results bolster the nascent research agenda focused on the importance of TVR on population dynamics. This research agenda can advance via both empirical investigations and population modelling studies. Empirically, there are still too few studies that test for the existence of TVR, perhaps because such studies require long-term data (Evers et al., 2021; Scott et al., 2021; Tenhumberg et al., 2018; van de Pol et al., 2016). Thus, we encourage researchers with long-term demographic data to explicitly test for TVR. A large literature on TVR would provide a better understanding of their prevalence and underlying mechanisms. Furthermore, our results are relevant to conservation research aimed at understanding and accurately forecasting the dynamics of populations known to be threatened by climate change (e.g. Compagnoni et al., 2021; Lindell et al., 2022). In the case of species particularly sensitive to climatic variation, explicit modelling of TVR could substantially change forecasts by correctly accounting for the indirect effects of climatic autocorrelation.

We have shown that populations that respond to a mix of temporal climate drivers can be buffered from increasing climate variance. We have also shown that climatic temporal autocorrelation, often acknowledged but unmodelled, can either increase or dampen the effect of variability when driven by mixed temporal climate drivers. Thus, explicitly accounting for mixed temporal climatic drivers might be an overlooked avenue to improve our understanding of population responses to future climatic change.

ORCID

Sanne M. Evers https://orcid.org/0000-0002-8002-1658
Tiffany M. Knight https://orcid.org/0000-0003-0318-1567
Aldo Compagnoni https://orcid.org/0000-0001-8302-7492

REFERENCES

Barraquand, F., & Yoccoz, N. G. (2013). When can environmental variability benefit population growth? Counterintuitive effects of nonlinearities in vital rates. *Theoretical Population Biology*, *89*, 1–11. https://doi.org/10.1016/j.tpb.2013.07.002

Bogdziewicz, M., Ascoli, D., Hacket-Pain, A., Koenig, W. D., Pearse, I., Pesendorfer, M., Satake, A., Thomas, P., Vacchiano, G., Wohlgemuth, T., & Tanentzap, A. (2020). From theory to experiments for testing the proximate mechanisms of mast seeding: An agenda for an experimental ecology. *Ecology Letters*, *23*(2), 210–220. https://doi.org/10.1111/ELE.13442

Boyce, M. S., Haridas, C. V., Lee, C. T., Boggs, C. L., Bruna, E. M., Coulson, T., Doak, D., Drake, J. M., Gaillard, J. M., Horvitz, C. C., Kali, & Tuljapurkar, S. D. (2006). Demography in an increasingly variable world. *Trends in Ecology & Evolution*, *21*(3), 141–148. https://doi.org/10.1016/j.tree.2005.11.018

Caswell, H. (2001). *Matrix population models: Construction, analysis, and interpretation* (2nd ed.). Sinauer Associates Inc.

Clark, J. S., Carpenter, S. R., Barber, M., Collins, S., Dobson, A., Foley, J. A., Lodge, D. M., Pascual, M., Pielke, R., Pizer, W., Pringle, C., Reid, W. V., Rose, K. A., Sala, O., Schlesinger, W. H., Wall, D. H., & Wear, D. (2001). Ecological forecasts: An emerging imperative. *Science*, *293*(5530), 657–660. https://doi.org/10.1126/science.293.5530.657

Compagnoni, A., Bibian, A. J., Ochocki, B. M., Rogers, H. S., Schultz, E. L., Sneck, M. E., Elderd, B. D., Iler, A. M., Inouye, D. W., Jacquemyn, H., & Miller, T. E. X. (2016). The effect of demographic

correlations on the stochastic population dynamics of perennial plants. *Ecological Monographs*, *86*(4), 480–494. https://doi.org/10.1002/ecm.1228

Compagnoni, A., Pardini, E., & Knight, T. M. (2021). Increasing temperature threatens an already endangered coastal dune plant. *Ecosphere*, *12*(3), e03454. https://doi.org/10.1002/ecs2.3454

Crone, E. E., Miller, E., & Sala, A. (2009). How do plants know when other plants are flowering? Resource depletion, pollen limitation and mast-seeding in a perennial wildflower. *Ecology Letters*, *12*(11), 1119–1126. https://doi.org/10.1111/j.1461-0248.2009.01365.x

Dahlgren, J. P., Bengtsson, K., & Ehrlén, J. (2016). The demography of climate-driven and density-regulated population dynamics in a perennial plant. *Ecology*, *97*(4), 899–907. https://doi.org/10.1890/15-0804.1

Di Cecco, G. J., & Gouhier, T. C. (2018). Increased spatial and temporal autocorrelation of temperature under climate change. *Scientific Reports*, *8*(1), 1–9. https://doi.org/10.1038/s41598-018-33217-0

Diggle, P. K. (1997). Extreme preformation in alpine *Polygonum viviparum*: An architectural and developmental analysis. *American Journal of Botany*, *84*(2), 154–169. https://doi.org/10.2307/2446077

Doak, D. F., Morris, W. F., Pfister, C., Kendall, B. E., & Bruna, E. M. (2005). Correctly estimating how environmental stochasticity influences fitness and population growth. *The American Naturalist*, *166*(1), E14–E21. https://doi.org/10.1086/430642

Eckhart, V. M., Geber, M. A., Morris, W. F., Fabio, E. S., Tiffin, P., & Moeller, D. A. (2011). The geography of demography: Long-term demographic studies and species distribution models reveal a species border limited by adaptation. *The American Naturalist*, *178*(Suppl. 1), S26–S43. https://doi.org/10.1086/661782

Evers, S. M., Knight, T. M., & Compagnoni, A. (2023). Data from: The inclusion of immediate and lagged climate responses amplifies the effect of climate autocorrelation on long-term growth rate of populations. *Zenodo*. https://doi.org/10.5281/zenodo.8026981

Evers, S. M., Knight, T. M., Inouye, D. W., Miller, T. E. X., Salguero-Gómez, R., Iler, A. M., & Compagnoni, A. (2021). Lagged and dormant season climate better predict plant vital rates than climate during the growing season. *Global Change Biology*, *27*(9), 1927–1941. https://doi.org/10.1111/gcb.15519

Fey, S. B., & Wieczynski, D. J. (2017). The temporal structure of the environment may influence range expansions during climate warming. *Global Change Biology*, *23*(2), 635–645. https://doi.org/10.1111/gcb.13468

Flores-Torres, A., & Montaña, C. (2012). Recruiting mechanisms of *Cylindropuntia leptocaulis* (Cactaceae) in the southern Chihuahuan Desert. *Journal of Arid Environments*, *84*, 63–70. https://doi.org/10.1016/J.JARIDENV.2012.04.006

Fritts, H. (2012). *Tree rings and climate*. Retrieved from https://books.google.com/books?hl=en&lr=&id=mkjsuFdwjeoC&oi=fnd&pg=PP1&ots=jZzjbSmJUH&sig=ATmC3iP2l-UcXhwXx_J1x4FKFEE

Heino, M., & Sabadell, M. (2003). Influence of coloured noise on the extinction risk in structured population models. *Biological Conservation*, *110*(3), 315–325. https://doi.org/10.1016/S0006-3207(02)00235-5

Hilde, C. H., Gamelon, M., Sæther, B. E., Gaillard, J. M., Yoccoz, N. G., & Pélabon, C. (2020). The demographic buffering hypothesis: Evidence and challenges. *Trends in Ecology & Evolution*, *35*(6), 523–538. https://doi.org/10.1016/j.tree.2020.02.004

Hindle, B. J., Pilkington, J. G., Pemberton, J. M., & Childs, D. Z. (2019). Cumulative weather effects can impact across the whole life cycle. *Global Change Biology*, *25*(10), 3282–3293. https://doi.org/10.1111/gcb.14742

Iler, A. M., Compagnoni, A., Inouye, D. W., Williams, J. L., Caradonna, P. J., Anderson, A., & Miller, T. E. X. X. (2019). Reproductive losses due to climate change-induced earlier flowering are not the primary threat to plant population viability in a perennial herb. *Journal of Ecology*, *107*(4), 1931–1943. https://doi.org/10.1111/1365-2745.13146

Iles, D. T., Rockwell, R. F., & Koons, D. N. (2019). Shifting vital rate correlations alter predicted population responses to increasingly variable environments. *The American Naturalist*, *193*(3), E57–E64. https://doi.org/10.1086/701043

Inouye, D. W. (1986). Long-term preformation of leaves and inflorescences by a long-lived perennial monocarp, *Frasera speciosa* (*Gentianaceae*). *American Journal of Botany*, *73*(11), 1535–1540. https://doi.org/10.1002/j.1537-2197.1986.tb10903.x

IPCC. (2014). Climate change 2014: Synthesis report. In Core Writing Team, R. K. Pachauri, & L. A. Meyer (Eds.), *Contribution of Working Groups I, II and III to the Fifth Assessment Report of the Intergovernmental Panel on Climate Change*. IPCC. https://doi.org/10.1177/0002716295541001010

Jäkäläniemi, A., Ramula, S., & Tuomi, J. (2013). Variability of important vital rates challenges the demographic buffering hypothesis. *Evolutionary Ecology*, *27*(3), 533–545. https://doi.org/10.1007/s10682-012-9606-y

Jones, O. R., Barks, P., Stott, I., James, T. D., Levin, S., Petry, W. K., Capdevila, P., Ch-eCastaldo, J., Jackson, J., Römer, G., Schuette, C., Thomas, C. C., & Salguero-Gómez, R. (2022). Rcompadre and rage—Two R packages to facilitate the use of the COMPADRE and COMADRE databases and calculation of life-history traits from matrix population models. *Methods in Ecology and Evolution*, *13*(4), 770–781. https://doi.org/10.1111/2041-210X.13792

Koons, D. N., Iles, D. T., Schaub, M., & Caswell, H. (2016). A life-history perspective on the demographic drivers of structured population dynamics in changing environments. *Ecology Letters*, *19*(9), 1023–1031. https://doi.org/10.1111/ele.12628

Lewontin, R. C., & Cohen, D. (1969). On population growth in a randomly varying environment. *Proceedings of the National Academy of Sciences of the United States of America*, *62*(4), 1056–1060. https://doi.org/10.1073/pnas.62.4.1056

Lindell, T., Ehrlén, J., & Dahlgren, J. P. (2022). Weather-driven demography and population dynamics of an endemic perennial plant during a 34-year period. *Journal of Ecology*, *110*(3), 582–592. https://doi.org/10.1111/1365-2745.13821

McDonald, J. L., Franco, M., Townley, S., Ezard, T. H. G., Jelbert, K., & Hodgson, D. J. (2017). Divergent demographic strategies of plants in variable environments. *Nature Ecology and Evolution*, *1*(2), 0029. https://doi.org/10.1038/s41559-016-0029

Morris, W. F., Altmann, J., Brockman, D. K., Cords, M., Fedigan, L. M., Pusey, A. E., Stoinski, T. S., Bronikowski, A. M., Alberts, S. C., & Strier, K. B. (2011). Low demographic variability in wild primate populations: Fitness impacts of variation, covariation, and serial correlation in vital rates. *The American Naturalist*, *177*(1), 14–28. https://doi.org/10.1086/657443

Morris, W. F., & Doak, D. F. (2004). Buffering of life histories against environmental stochasticity: Accounting for a spurious correlation between the variabilities of vital rates and their contributions to fitness. *The American Naturalist*, *163*(4), 579–590.

Morris, W. F., Pfister, C. A., Tuljapurkar, S., Haridas, C. V., Boggs, C. L., Boyce, M. S., Bruna, E. M., Church, D. R., Coulson, T., Doak, D. F., Forsyth, S., Gaillard, J., Horvitz, C. C., Kalisz, S., Kendall, B. E., Knight, T. M., Lee, C. T., & Menges, E. S. (2008). Longevity can buffer plant and animal populations against changing climate variability. *Ecology*, *89*(1), 19–25. https://doi.org/10.1890/07-0774.1

Neubert, M. G., & Caswell, H. (2000). Density-dependent vital rates and their population dynamic consequences. *Matrix*, *121*(34), 103–121.

Noël, F., Maurice, S., Mignot, A., Glémin, S., Carbonell, D., Justy, F., Guyot, I., Olivieri, I., & Petit, C. (2010). Interaction of climate, demography and genetics: A ten-year study of *Brassica insularis*, a narrow endemic Mediterranean species. *Conservation Genetics*, *11*(2), 509–526. https://doi.org/10.1007/s10592-010-0056-1

Paniw, M., Ozgul, A., & Salguero-Gómez, R. (2018). Interactive life-history traits predict sensitivity of plants and animals to

temporal autocorrelation. *Ecology Letters*, *21*(2), 275–286. https://doi.org/10.1111/ele.12892

Pilowsky, J. A., & Dahlgren, J. P. (2020). Incorporating the temporal autocorrelation of demographic rates into structured population models. *Oikos*, *129*(2), 238–248. https://doi.org/10.1111/oik.06438

R Core Team. (2021). *R: A language and environment for statistical computing*. Retrieved from https://www.r-project.org/

Salguero-Gómez, R., Jones, O. R., Jongejans, E., Blomberg, S. P., Hodgson, D. J., Mbeau-Ache, C., Zuidema, P. A., de Kroon, H., & Buckley, Y. M. (2016). Fast-slow continuum and reproductive strategies structure plant life-history variation worldwide. *Proceedings of the National Academy of Sciences of the United States of America*, *113*(1), 230–235. https://doi.org/10.1073/pnas.1506215112

Schwager, M., Johst, K., & Jeltsch, F. (2006). Does red noise increase or decrease extinction risk? Single extreme events versus series of unfavorable conditions. *The American Naturalist*, *167*(6), 879–888. https://doi.org/10.1086/503609

Scott, E. R., Uriarte, M., & Bruna, E. M. (2021). Delayed effects of climate on vital rates lead to demographic divergence in Amazonian forest fragments. *Global Change Biology*, *28*, 2021.06.28.450186. https://doi.org/10.1111/gcb.15900

Stubben, C., Milligan, B., & Maintainer, P. N. (2016). *Package 'popbio' documentation.*

Stubben, C. J., & Milligan, B. G. (2007). Estimating and analyzing demographic models using the popbio package in R. *Journal of Statistical Software*, *22*(11), 1–23. https://doi.org/10.18637/jss.v022.i11

Tei, S., Sugimoto, A., Yonenobu, H., Matsuura, Y., Osawa, A., Sato, H., Fujinuma, J., & Maximov, T. (2017). Tree-ring analysis and modeling approaches yield contrary response of circumboreal forest productivity to climate change. *Global Change Biology*, *23*(12), 5179–5188. https://doi.org/10.1111/gcb.13780

Tenhumberg, B., Crone, E. E., Ramula, S., & Tyre, A. J. (2018). Time-lagged effects of weather on plant demography: Drought and *Astragalus scaphoides*. *Ecology*, *99*(4), 915–925. https://doi.org/10.1002/ecy.2163

Tredennick, A. T., Teller, B. J., Adler, P. B., Hooker, G., & Ellner, S. P. (2018). Size-by-environment interactions: A neglected dimension of species' responses to environmental variation. *Ecology Letters*, *21*(12), 1757–1770. https://doi.org/10.1111/ELE.13154

Trugman, A. T., Anderegg, L. D. L., Anderegg, W. R. L., Das, A. J., & Stephenson, N. L. (2021). Why is tree drought mortality so hard to predict? *Trends in Ecology & Evolution*, *36*(6), 520–532. https://doi.org/10.1016/J.TREE.2021.02.001

Tuljapurkar, S. (1990). Population dynamics in variable environments. In *Lecture notes in biomathematics*. Springer. https://doi.org/10.1007/978-3-642-51652-8

Tuljapurkar, S., & Haridas, C. V. (2006). Temporal autocorrelation and stochastic population growth. *Ecology Letters*, *9*(3), 327–337. https://doi.org/10.1111/j.1461-0248.2006.00881.x

Urban, M. C., Bocedi, G., Hendry, A. P., Mihoub, J. B., Pe'er, G., Singer, A., Bridle, J. R., Crozier, L. G., De Meester, L., Godsoe, W., Gonzalez, A., Hellmann, J. J., Holt, R. D., Huth, A., Johst, K., Krug, C. B., Leadley, P. W., Palmer, S. C., Pantel, J. H., Schmitz, A., … Travis, J. M. J. (2016). Improving the forecast for biodiversity under climate change. *Science*, *353*(6304), aad8466. https://doi.org/10.1126/science.aad8466

van de Pol, M., Bailey, L. D., McLean, N., Rijsdijk, L., Lawson, C. R., & Brouwer, L. (2016). Identifying the best climatic predictors in ecology and evolution. *Methods in Ecology and Evolution*, *7*(10), 1246–1257. https://doi.org/10.1111/2041-210X.12590

Vasseur, D. A., DeLong, J. P., Gilbert, B., Greig, H. S., Harley, C. D. G., McCann, K. S., Savage, V., Tunney, T. D., & O'Connor, M. I. (2014). Increased temperature variation poses a greater risk to species than climate warming. *Proceedings of the Royal Society B: Biological Sciences*, *281*(1779), 20132612. https://doi.org/10.1098/rspb.2013.2612

Vázquez, D. P., Gianoli, E., Morris, W. F., & Bozinovic, F. (2017). Ecological and evolutionary impacts of changing climatic variability. *Biological Reviews*, *92*(1), 22–42. https://doi.org/10.1111/brv.12216

Westerband, A. C., & Horvitz, C. C. (2017). Early life conditions and precipitation influence the performance of widespread understorey herbs in variable light environments. *Journal of Ecology*, *105*(5), 1298–1308. https://doi.org/10.1111/1365-2745.12757

SUPPORTING INFORMATION

Additional supporting information can be found online in the Supporting Information section at the end of this article.

Supinfo S1. Method details

S1.1. Simulating temporal sequences

S1.2. Calculating vital rate distributions

S2. Additional results

S2.1. Life history trait distributions and responses

S2.2. Different climate signal strengths between vital rates

S2.3. Regression summaries

S2.4. Individual life histories results